(**Fig. 3b**). Membrane fusion activity for optimized MEND was increased compared to initial MEND at acidic pH. On the other hand, the apparent pKa of optimized MEND was comparable to that of the initial MEND (**Fig. 3a**). Factor VII is a secreted protein that can be readily measured in plasma, providing an index for the level of target gene knockdown in liver[24,33]. Therefore, we evaluated Factor VII knockdown using MENDs. As shown in **Fig. 3c** and **3d**, initial and optimized MENDs decreased both liver mRNA and plasma level of Factor VII protein in a dose-dependent manner, with ED50s of approximately 0.8 mg/kg and 0.06 mg/kg (initial and optimized MENDs, respectively) for plasma levels of Factor VII. The results suggested that optimized MEND successfully induced the efficient knockdown in liver after systemic administration in mice. Next, the durability of knockdown of plasma Factor VII was determined. Single injection of optimized MEND was capable of mediating knockdown for at least 14 days at 50% inhibition (**Fig. 3e**). Finally, the distribution of siRNA was observed in the livers of animals treated with optimized MEND encapsulating Cy5-labeled siRNA. As shown in **Fig 3f**, MEND uniformly delivered siRNA to parenchymal cells in liver. These results suggested that optimized MENDs loaded with HCV-targeting dh-siRNAs can induce silencing against cytosolic replicating HCV. Therefore, further investigation was performed using the optimized MEND.

Silencing infectious HCV *in vivo*. We recently demonstrated the use of a novel mouse model for *in vivo* infection with hepatitis viruses[34] (**Fig. 4a**). Specifically, the model consisted of severe combined immunodeficient (SCID) mice, transgenic for urokinase-type plasminogen activator (uPA), which were transplanted with human hepatocytes. (In the following text, this model will be referred to simply as "chimeric mice".) We also have reported that these chimeric mice are a robust animal model to evaluate the efficacy of interferon and other anti-HCV agents[35].

First, optimized MENDs encapsulating DY547-labeled siRNAs were administered intravenous (IV) to chimeric mice (**Fig. 4b**). After 30 minutes, accumulation of siRNA was observed in the livers of the chimeric mice. We noted that the intracellular distribution of siRNA was not patchy, but was instead diffusely organized in the cytoplasm, presumably reflecting endosomal escape following endocytosis[21].

Both the efficacy and tolerability of these dh-siRNA-loaded optimized MENDs are critical issues for potential human clinical usage. Therefore, we examined the toxicology (in the "humanized" livers of chimeric mice) of optimized MEND-siRNAs during repeat-dose administration. Specifically, dh-siRNAs were formulated in optimized MENDs and administered to chimeric mice for a total of four IV infusions (on days 0, 2, 4, and 6) at siRNA doses of 1 mg/kg (**Fig. 4a**). This treatment appeared to be well tolerated; human hepatocytes in the chimeric mice remained viable, as demonstrated by tracking of serum human albumin levels and serum alanine aminotransferase (ALT) levels (an indicator of liver toxicity) (**Fig. 4c** and **4d**). Although a slight increase in ALT values was observed, the change was not additive over the course of successive infusions. (**Fig. 4d**). Consistent with the results, a mixture of the dh-si197-1, dh-si197-6, and dh-si50-10 (siHCVs) provided silencing of HCV replication (**Fig. 4e**). In contrast, a non-targeting control siRNA (siControl), also formulated in optimized MENDs, did not induce silencing of HCV replication (**Fig. 4e**). To evaluate the long-term efficacy of dh-siRNA-mediated silencing of HCV replication, we dosed chimeric mice with combined (three siRNAs; administered as IV infusions on days 0 and 3) and followed the animals for 2 weeks (**Fig. 5a**). As seen above for knockdown duration by systemic optimized MEND treatment (**Fig. 3c**), the combined siHCVs (dh-si197-1, dh-si197-6, and dh-si50-10, also formulated in optimized MENDs) suppressed HCV replication for 2 weeks (**Fig. 5b**); no adverse effects were seen in human serum albumin levels or body weights (**Fig. 5c**). At day 14, livers were also harvested and screened by immunohistochemistry (IHC) and for quantitation (via real-time RT-PCR) of hepatic HCV RNA. As shown in **Figure 5d**, intrahepatic HCV core protein (detected by IHC) was dramatically reduced by the siHCV treatment (PXB283-27 mouse) compared with the siControl treated mouse, in which HCV core protein was detected within human hepatocytes. RT-PCR[36] demonstrated that the siHCV treatment provided an approximately 25-fold reduction in hepatic HCV RNA levels (treatment vs. siControl; 1.34×10^3 vs. 3.36×10^4 copies/μg total RNA, respectively).

Separate experiments, using another HCV pathogenesis mouse model[37], demonstrated that siHCV (dh-si197-1) treatment improved HCV-induced liver inflammatory responses in conditional HCV transgenic mice (**Fig. 5e**).

Discussion

The distinct effector phase of the RNAi pathway has been the focus of considerable research. This step depends on cleavage of the target mRNA by the RISC following base-pairing with the antisense strand of siRNA[38]. Therefore, the prediction of an effective siRNA had been evaluated based on the molecular mechanism of RISC assembly or the sequence preferences of the RISC endonuclease. Numerous strategies have been published to select siRNA sequences for targeting endogenous mRNA, and the resulting sequences have proved effective in some applications. However, the concept may not be appropriate to select target genes from other organisms, such as viruses.

Viruses typically exist as populations harboring multiple sequence variants, making these organisms notorious for the ability to develop resistance and escape control. Thus the prediction of effective antiviral siRNAs requires additional factors such as conservation of target sequence preferences. Based the level of sequence conservation among different HCV genotypes, the IRES of the 5′ UTR has been proposed as an RNAi target site. As highly conserved sequences are likely to contain structurally or functionally constrained elements, it has been argued that local higher order structures in target mRNAs might restrict accessibility to RISC, and attenuate or abolish RNAi activity. There are reports that the secondary structure of target sites in mRNAs strongly reduce siRNA-mediated RNAi activity[16,17], hence the accessibility of certain local target structures on the mRNA is an important determinant in the gene silencing ability of siRNAs[18]. However, in general, RNA folding program such as mfold or sfold can predict more than one secondary structures for the same mRNA; it is difficult to know which of the proposed structures represents the real or the most frequent fold employed in the cell. Therefore, target mRNA structure is a criterion that cannot be easily defined nor confidently scored solely on the bases of *in silico* calculations.

To facilitate the prediction of highly active siRNA molecules in the HCV structurally elements, we used human Dicer endoribonuclease activity for preparation of certain siRNAs. Because RISC loading takes place in the context of the RISC-loading complex, which consists of an Argonaute protein, Dicer, and the dsRBD-containing protein TRPB in human cells[39], Dicer favorable siRNA preference might be influence on loading to the complex. With mapping the corresponding cleavage site by the endoribonuclease-prepared siRNAs with the long dsRNA of IRES region, potent siRNA candidates in the structurally element have been identified by 5′ RACE methods. Thereby, we speculate that the accessibility of Dicer to target mRNA also may be a critical factor. Indeed, siRNA sequences derived by our hunting-by-Dicer method may be more potent inducers of RNAi than the siRNAs predicted by commercial design software.

The optimized MEND was accumulated in liver to around 90% of the injected dose within 30 min (data not shown). Recently, it was reported that neutral liposomal systems acquire ApoE in circulation, which enhances uptake of the liposomes into hepatocytes by low-density lipoprotein (LDL) receptor (LDLR) expressed on the surface

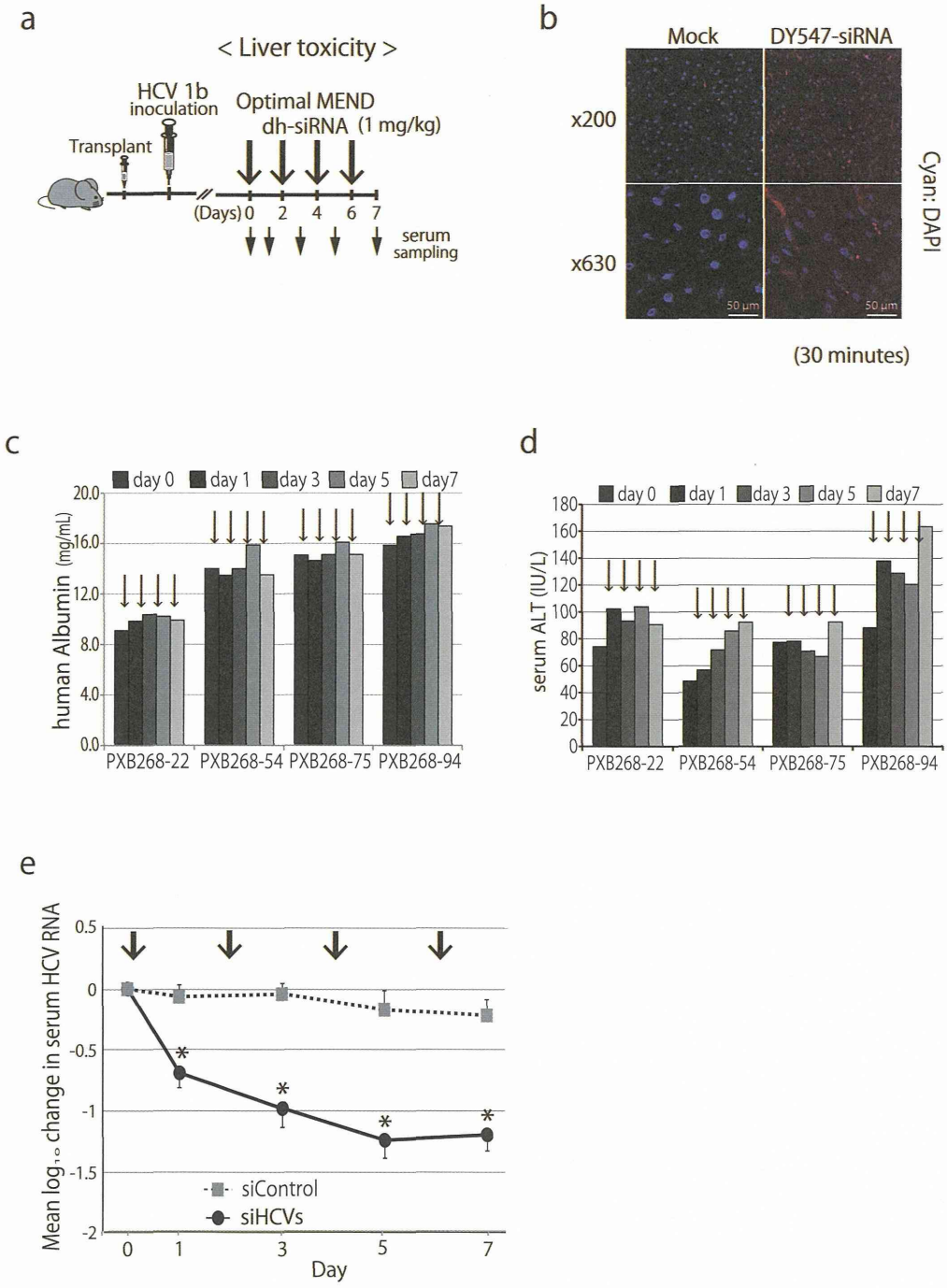

Figure 4 | Liver toxicity of siRNA formulated in optimized MEND in humanized chimeric mouse. (a) Schedule of treatment by dh-siRNA formulated in optimized MENDs in chimeric mice carrying human hepatocytes (PXB mice) infected with HCV genotype 1b (HCR6). The mice were administered intravenously with siRNA-loaded optimized MENDs by 4 repeat doses. All optimized MENDs were loaded with siRNA and administered to provide doses of 1 mg/kg. (b) Distribution characteristics of siRNA in chimeric mice carrying human hepatocytes. DY-547-labeled siRNA formulated in optimized MENDs was injected intravenously into the orbital veins of chimeric mice. The liver was observed by fluorescence microscopy at 30 min after injection. The nuclei were stained with DAPI. Mock: unlabeled siRNA formulated in optimized MEND. (c, d) Liver toxicity by administration of siHCVs (the HCV-specific dh-siRNAs formulated in optimized MEND). Four-time injection of siRNA formulated in optimized MEND into HCV-infected chimeric mice (individual animals: PXB268-22, PXB268-54, PXB268-75, and PXB268-94) was performed on days 0, 2, 4, and 6 (indicated by vertical arrows). Serum human albumin levels (c) and alanine aminotransferase (ALT) levels (d) were monitored for 1 week. (e) Four-time injection of siHCVs and siControl into HCV-infected chimeric mice was performed on days 0, 2, 4, and 6 (indicated by vertical arrows). The HCV genomic RNA change from baseline following treatment with siHCVs (n=4) or with siControl (non-targeting control siRNA formulated in optimized MEND, n=3) were shown; data points are presented as the mean ± s.d.

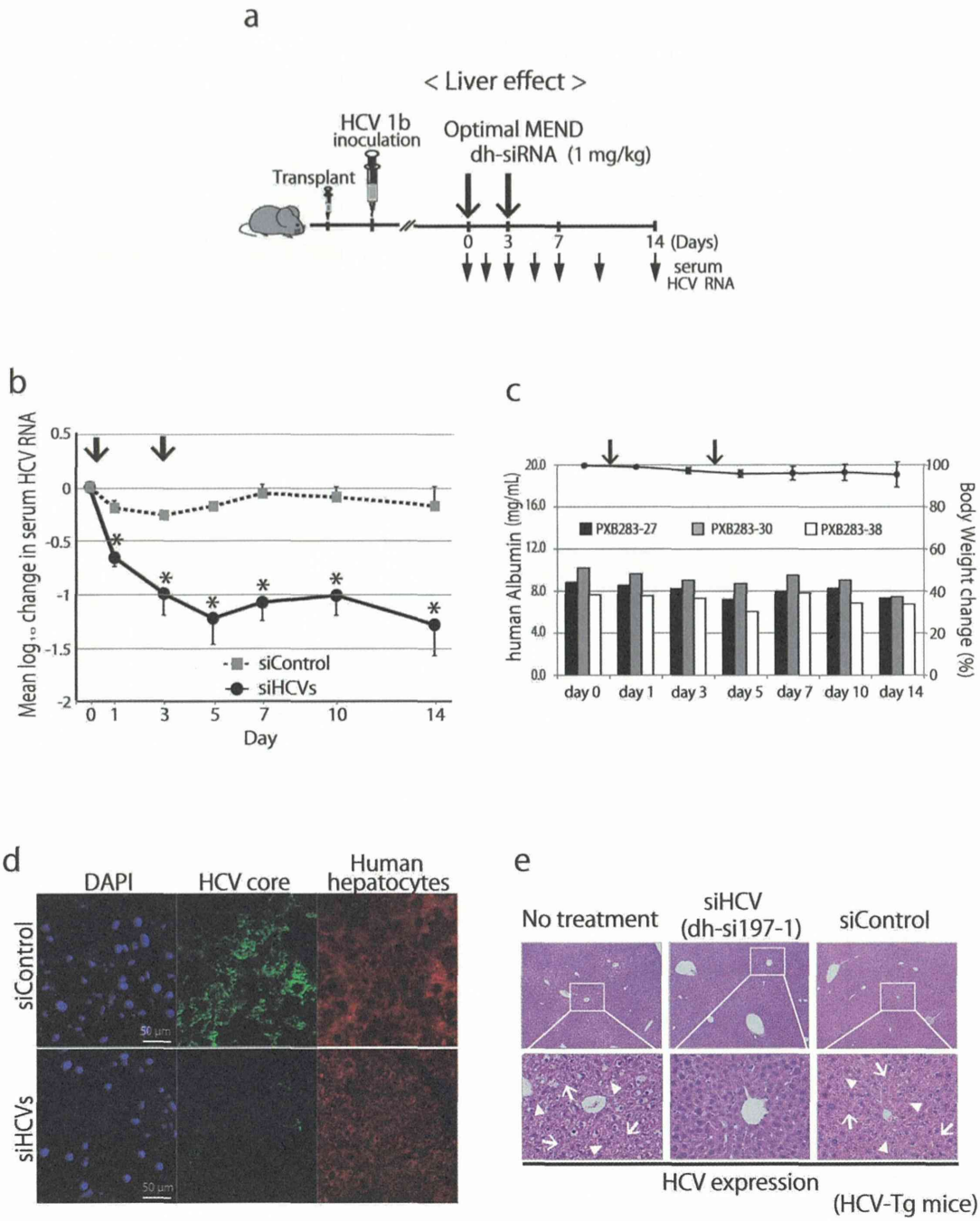

Figure 5 | Silencing efficacy of siRNA formulated in optimized MEND against ongoing infectious HCV RNA. (a) Schedule of treatment by dh-siRNA formulated in optimized MENDs in chimeric mice carrying human hepatocytes (PXB mice) infected with HCV genotype 1b (HCR6). The mice were administered intravenously with siRNA (1 mg/kg)-loaded optimized MENDs by 2 repeat doses. (b) Long-term silencing efficacy of siHCVs (the HCV-specific dh-siRNAs formulated in optimized MEND) against ongoing infectious HCV RNA. The HCV genomic RNA change from baseline in individual mice following treatment with siHCVs (n=3) or with siControl (n=3) were monitored for 2 weeks. (c) The serum human albumin levels (indicated as bar in left y-axis) in individual animals, as well as the change of body weight (indicated as line in right y-axis; plotted as mean + s.d. (across 3 animals)) over 2 weeks. (d) Intrahepatic analysis of chimeric mice infected with HCV. Two weeks after administration of siHCVs or siControl (injected on day 0 and day 3), chimeric mouse liver was harvested. The presence of human hepatocytes and HCV core protein were evaluated by immunohistochemistry. (e) dh-siRNA-mediated amelioration of HCV-induced liver damage in a murine model of inducible HCV. The inducible-HCV transgenic mouse model (HCV-Tg mice; see Materials and Methods) provides conditional expression of HCV core, E1, E2, and NS2 proteins. Six months after HCV induction, mice were treated by injection (on days 0 and 2) with optimized MENDs loaded with a single species of dh-siRNA (si197-1). On day 4, livers were harvested and assessed histologically (hematoxylin and eosin staining) for HCV-induced liver inflammatory responses. Degenerated liver tissue with diffuse inflammation and spotty necrosis was observed in the livers of the "no treatment" and siControl mice; treatment with si197-1-loaded optimized MENDs reduced HCV-induced liver damage. Arrows indicate necrosis; arrowheads indicate inflammation.

www.nature.com/scientificreports

of hepatocytes[40,41]. It also was reported that the average diameters of sinusoidal fenestrae in C57CL/B mice and healthy human are 141 nm and 107 nm, respectively[42]. The average diameter of optimized MENDs was around 80 nm (**Fig. 3a**), which would permit optimized MENDs to pass through fenestrae and access hepatocytes. Therefore, we assume that MENDs containing YSK05 are taken up by hepatocytes by a process mediated by ApoE-LDL receptor association. This association presumably follows extravasation of MENDs from sinusoidal lumen to Disse through fenestrae, which results in widespread delivery of siRNAs to hepatocytes in healthy and transgenic mice, as well as to human hepatocytes in chimeric mice. The lipid composition for the initial MEND *in vivo* was chosen at YSK05/DSPC/cholesterol/PEG-lipid=50 : 10 : 40 : 3 mol%, as described previously[24,43]. Since DSPC, a helper lipid, was not essential to exert silencing in liver, DSPC was eliminated from lipid envelope (**supplementary Fig. 2a**). The pH-sensitive YSK05 lipid is presumed to be responsible for the endosomal release of the MEND cargo. Hence we tested the silencing activity of siRNA-loaded MENDs with increasing ratios of YSK05; activity was maximized at approximately 70 mol% YSK05. Based on our testing, a MEND composed of YSK05, cholesterol, and PEG-lipid at 70 : 30 : 3 was regarded as the optimized version. For systemic siRNA delivery using ionizable LNPs, lipid pKa value was identified as an important parameter, with optimum pKa in the range of 6.2–6.5[44]. In the present study, the pKa values of initial and optimized MENDs were determined as 6.6 and 6.4 respectively, which fell within this optimal pKa range. The endosomal escape of MEND is presumably mediated by membrane fusion. According to hemolysis activity, optimization of MEND improved fusion ability at acidic pH, but did not affect fusion at neutral pH. This optimization contributed to a 10-fold increase in silencing activity, yielding an ED50 of ~0.06 mg/kg in liver. Our results suggested that efficient siRNA delivery depends on the use of lipid-based nano-carriers that provide both optimized pKa and highly fusogenic characteristics. We also successfully delivered anti-miRNA oligonucleotide against miRNA-122 (miR-122) into hepatocytes using optimized YSK05-MEND, which resulted in efficient miR-122 knockdown and reduced plasma cholesterol level[45,46]. Our results permitted us to attempt delivery of dh-siRNAs to HCV-infected liver using the optimized MENDs. Our steady progress with a liver-targeting delivery system should facilitate the development of a safe and effective strategy for targeting HCV in hepatocytes in the near future.

Although our results were conducted in mouse models for HCV pathogenesis, results from these technologies are expected to provide therapeutic potential against infectious HCV *in vivo*, while also providing a new siRNA design tool for targeting viral seqeunces. Despite other obstacles (e.g., off-target effects), RNAi using these technologies provides a new potential therapeutic application that may effectively treat HCV infection.

Methods

Ethics statements. All *in vivo* experiments were approved by the Institutional Animal Care and Use Committee, and protocols for animal experiments were approved by the local ethics committee. The animals received humane care according to guidelines of the National Institutes of Health. Human patients provided informed written consent before sampling (collection of HCV-containing blood samples).

siRNAs. The design of HCV-directed siRNAs has been described previously[26]. Briefly, we designed nine siRNAs that target the 5′-UTR and 3′-UTR of the HCV genome and examined their efficacy in the *in vitro* inhibition of HCV replication. Of these nine siRNAs, the most effective siE was one directed toward nucleotides 323 to 342 of the HCV genome. The sequences for the sense and antisense strands of the siRNA are as follows: siE sense: 5′-GUC UCG UAG ACC GUG CAU CAU U-3′; antisense: 5′-UGA UGC ACG GUC UAC GAG ACU U-3′. siRNAs were generated by annealing equimolar amounts of complementary sense and antisense strands.

Anti-luciferase siRNA (siLuc) (sense: 5′-CCG UCG UAU UCG UGA GCA ATT-3′; antisense: 5′-UUG CUC ACG AAU ACG ACG GTT-3′) was purchased from Sigma (Ishikari, Japan). Anti-FVII siRNA (siFVII) (sense: 5′-GGAucAucucAA-GucuuAcT*T-3′; antisense: 5′-GuAAGAcuuGAGAuGAuccT*T-3′; lower case letters indicate 2′-fluoro-modified nucleotides, asterisks indicate phosphorothioate linkages) were purchased from Hokkaido System Science Co., Ltd. (Sapporo, Japan).

Dicer-generated siRNAs. We generated the HCV-specific long dsRNA template for *in vitro* transcription by PCR-amplified DNA templates and synthesized Dicer-generated siRNAs (d-siRNAs) by cleavage with recombinant human Dicer (rhDicer; Gene Therapy Systems, San Diego, CA)[26]. By comparison with the silencing efficiency of d-siRNAs, d-siD5-50 and d-siD5-197 silenced the HCV replication more efficiently than synthetic siE (Supplementary information Fig. 1). The template dsRNAs of d-siD5-50 and d-siD5-197 were located at nucleotides 309–358 and 199-395 of HCR6 sequence (GenBank accession number AY045702).

siRNAs predicted by the commercial software. The siRNA design algorithms for antiviral RNAi, siVirus, siDirect and Block-iT (Invitrogen), were used for the selection of the target sequence for siRNA within the specified target HCV genome (nucleotides 199–395).

Cell culture and HCV-replicon assay. We used four HCV subgenomic replicon cell lines, FLR3-1 (genotype 1b, Con-1)[47], R6FLR-N (genotype 1b, strain N)[26], JFH-1/FLR/K4 (genotype 2a)[48], and RMT-tri (genotype 1a)[49], which have the firefly luciferase gene for the sensitive and precise quantification of the HCV replication levels using a luciferase assay. We also used REF cells[30] which harbor the divided-full genome replicon for analysis of the HCV 5′ UTR sequences. Each cell line was seeded at a density of 5×10^3 per well in 96-well tissue culture plates, and grown (at 37°C and 5% CO_2) in complete Dulbecco's modified Eagle's medium supplemented with Glutamax I (Invitrogen, Carlsbad, CA) and containing 5% fetal calf serum (Invitrogen). Cells were transfected with 30 nM siRNA using RNAiMax (Invitrogen, Carlsbad, CA). After 72 hours, luciferase activity was determined in triplicate using the Steady-Glo or Bright-Glo luciferase assay kit (Promega Madison, WI). The luciferase signal was measured using an LB940 luminometer (Berthold, Freiburg, Germany) and the results were expressed as the mean percentage of control. IC_{50} values of siRNA were calculated by nonlinear curve-fitting using the equation: $Y=100-(Y_{Bottom} \times X/(IC_{50} + X))$, where Y represents percent inhibition and X represents the concentration of siRNAs.

5′-rapid amplification of cDNA ends (RACE) analysis. Replicon cells were transfected with synthetic HCV-specific siRNA (siE) and Dicer-generated siRNAs using Lipofectamine RNAiMAX or Lipofectamine 2000 (Invitrogen) according to the manufacturer's protocol. At 6 h post-transfection, total RNA from replicon cells was extracted using the acid guanidinium-phenol-chloroform method[26].

For the RNA oligo ligation method, 5 μg of total RNA was ligated to the GeneRacer RNA adapter (Invitrogen, 5′-CGA CUG GAG CAC GAG GAC ACU GAC AUG GAC UGA AGG AGU AGA AA-3′) without any prior processing. Ligated RNA was reverse transcribed into cDNA using the HCV-specific reverse primer (R6 876-R20 reverse primer: 5′- AGA GGA AGA TAG AGA AAG AG-3′). To detect cleavage product, semi-nested-PCR was performed as follows: first-run PCR used a primer complementary to the RNA adapter (GeneRacer 5′ Nested Primer: 5′-GGA CAC TGA CAT GGA CTG AAG GAG TA-3′) in combination with an HCV-specific primer (R6 610-R24 reverse primer: 5′-CCC TCG TTG CCA TAG AGG GGC CAA-3′); second-run PCR used the same oligo specific primer (GeneRacer 5′ Nested Primer) in combination with a second HCV-specific primer (R6 536-R20 reverse primer: 5′-GAT AGG TTG TCG CCT TCC AC-3′).

For the C-tailing at the 3′-end of RNA method, first-strand cDNA synthesis was performed by using SuperScript II reverse transcriptase (Promega Corporation, Madison, WI) to transcribe total RNA (5 μg) with the HCV-specific reverse primer (R6 876-R20 reverse primer) according to the manufacturer's protocol. The resulting first-strand cDNA was subjected to another round of 5′-RACE using a distinct RACE kit (Cat. 18374-058, Invitrogen, Carlsbad, CA). The first-strand cDNA was tailed at the 3′-end by terminal transferase TdT and dCTP. The primer set consisted of an HCV-specific reverse primer (R6 610-R24) and the Abridged Anchor Primer for the first-run PCR, and an HCV-specific reverse primer (R6 536-R20) and the Abridged Universal Amplification Primer for the second-run PCR.

Amplification fragments obtained by the two independent 5′-RACE methods were resolved on 3.0% agarose and sized using a 1-kb Plus DNA Ladder (Invitrogen). Specific cleavage sites were further confirmed by DNA sequencing.

Dicer-hunting siRNA sequences design. Based on the cleavage site defined by d-siRNAs, reverse genetic approach was applied to the design of Dicer favourable siRNA sequence. A dh-siRNA consists of duplexes of 21-nt RNAs that are base-paired with 2-nt 3′ overhangs.

Preparation of MENDs. Cholesterol, 1,2-distearoyl-sn-3-phosphatidylcholine (DSPC), 1,2-dimyristoyl-sn-glycerol, and methoxyethyleneglycol 2000 ether (PEG-DMG) were purchased from Avanti Polar Lipid (Albaster, AL). The synthesis of YSK05 was performed as previously described[21]. MENDs encapsulating siRNAs were prepared by a *t*-BuOH dilution procedure. Lipid in 90% (v/v) *t*-BuOH was mixed with siRNA in 20 mM citrate buffer (pH 4.0) at siRNA/lipid ratio of 0.1 (wt/wt) under strong agitation to yield a final *t*-BuOH concentration of 60% (v/v). Then, the lipid/siRNA mixture was added into 20 mM citrate buffer (pH 4.0) under strong agitation to yield a final *t*-BuOH concentration of <12% (v/v). Ultrafiltration was performed to remove *t*-BuOH, replacing external buffer with phosphate-buffered saline (PBS, pH7.4) and concentrating the MENDs. A lipid envelope of initial MEND was

prepared using YSK05, DSPC, cholesterol, and PEG-DMG at a molar ratio of 50 : 10 : 40 : 3 as described previously[24,43], and optimized MEND was prepared using YSK05, cholesterol, and PEG-DMG at a molar ratio of 70 : 30 : 3.

Characterization of MEND. The average diameter and zeta-potential of MENDs were determined using a Zetasizer Nano ZS ZEN3600 (MALVERN Instrument, Worcestershire, UK). siRNA encapsulation efficiency was determined by a RiboGreen assay (Invitrogen Carlsbad, CA). MENDs were diluted in 10 mM HEPES buffer (pH 7.4) containing 20 μg/mL dextran sulfate and Ribogreen in the presence or absence of 0.1% (w/v) Triton X-100. Fluorescence was measured by Varioskan Flash (Thermo scientific) with λex=500 nm, λem=525 nm. siRNA concentration was calculated based on a siRNA standard curve. siRNA encapsulation efficiency was calculated by comparing siRNA concentration in the presence and absence of Triton X-100. The pKa of YSK05 in each MEND was determined using 6-(p-Toluidino)-2-naphthalenesulfonic acid (TNS). Thirty μM of MEND lipid and 6 μM of TNS were mixed in 200 μL of 20 mM citrate buffer, 20 mM sodium phosphate buffer, or 20 mM Tris-HCl buffer, containing 130 mM NaCl at a pH ranging from 3.0 to 9.0. Fluorescence was measured by a Varioskan Flash with λex=321 nm, λem=447 nm, at 37°C. The pKa values were measured as the pH giving rise to half-maximal fluorescent intensity.

Hemolysis assay. Fresh red blood cells (RBCs) were collected from ICR mice and suspended in PBS. The RBC suspension was mixed with indicated amount of MEND, incubated at 37°C for 30 min, and then centrifuged (4°C, 400 *g*, 5 min). The absorbance of the supernatant was measured at 545 nm. Positive and negative control samples were prepared by incubation of RBCs with 0.5% (wt/v) Triton X-100 or PBS (respectively). The %hemolysis was epressed as the % of the absorbance of the positive control.

***In vivo* mouse Factor VII knockdown experiments.** Male ICR mice (5–6 weeks old) were purchased from Japan SLC (Shizuoka, Japan). MENDs encapsulating siFVII were diluted to the appropriate concentrations in PBS (pH 7.4) and administered intravenously (IV; via the tail vein) at a dose volume of 10 to 15 mL/kg. At the indicated time points, blood and liver were collected. The blood was processed to plasma, and plasma levels of Factor VII protein were determined using a colorimetric Biophen VII assay kit (Aniara) according to the manufacturer's protocol. The standard curve for Factor VII plasma levels was generated using plasma collected from PBS-treated mice. Total RNA in liver was isolated using TRIzol (Invitrogen) according to the manufacturer's protocol. The resulting RNA was reverse transcribed using a High Capacity RNA-to-cDNA kit (ABI) according to manufacturer's protocol. For each specimen, quantitative PCR analysis was performed on 2 ng of cDNA using Fast SYBR Green Master Mix (ABI) and a Lightcycler480 system II (Roche). All reactions were performed in a volume of 15 μL. The primers for mouse *fvii* were (forward) 5′-TCG AAT CCA TGT CAG AAC GGA GGT -3 and (reverse) 5′-CCG ACC CTC AAA GTC TAG GAG GCA-3′.

***In vivo* microscopic observation.** Optimized MENDs encapsulating Cy5-labeled siRNA were administered into male ICR mice (5–6 weeks old). Five min before projected sacrifice, FITC-conjugated isolectin B4 (40 μg/mouse) was intravenously injected via the tail vein to stain blood vessels. At 30 min after intravenously injection of optimized MEND, each animal was perfused with PBS to remove blood from the liver, then with 4% paraformaldehyde (PFA)-PBS for fixation. Liver tissues were excised and further fixed with 4% PFA-PBS for 24 hr at 4°C, then submerged in 20% sucrose-PBS for 4 hr at 4°C. The liver was embedded in OCT compound (Sakura Fine Technical, Tokyo, Japan) and snap-frozen in liquid nitrogen. Frozen samples were cut in 30 μm-thick sections (LEICA CM3000, Leica Microsystems, Wetzlar, Germany). The samples were stained with Hoechst33342 to detect nuclear DNA, and observed at an excitation wavelength of 633 nm using a laser-equipped Nikon A1 (Nikon Co. Ltd., Tokyo, Japan) with a x60 objective lens.

***In vivo* HCV infection experiments.** We purchased chimeric mice from PhenixBio (Hiroshima, Japan). The chimeric mice were generated by transplanting human primary hepatocytes into severe combined immunodeficient (SCID) mice carrying the urokinase plasminogen activator transgene controlled by an albumin promoter (uPA/SCID)[34]. Six weeks after hepatocyte transplantation, each mouse was injected IV with patient serum containing 10^6 copies of HCV genotype 1b (HCR6; accession number AY045702)[36]. HCV inoculations, drug administration, blood collection, and sacrifice were performed under ether anesthesia. Blood samples were taken from the orbital vein and sera were immediately isolated. Human serum albumin in the blood of chimeric mice was measured with a commercially available kit (Alb-II kit; Eiken Chemical, Tokyo, Japan) and serum ALT level was determined with enzymatic assays (Horiba ABX Diagnostics) according to the manufacturer's instructions[35].

Rhodamine-labeled siRNA was synthesized by Dharmacon (Lafayette, CO). Alexa-546 or Alexa-568 labeled siE/CL-LA was injected IV into BALB/c mice. After 30 minutes, the liver, lung, spleen, and kidney were harvested from each mouse. Sections of these tissues then were stained with DAPI (Molecular Probes) and slides examined using confocal laser microscopy (Zeiss).

Liver tissues obtained from mice were embedded in OCT compound (Ted Pella, Redding, CA). The frozen tissues were cut into thin sections (6 μm) and placed on glass slides. The sections were fixed in 10% buffered formalin and then treated with 0.1% Triton X-100. To detect HCV protein by immunohistochemistry (IHC)[35], the slides were incubated with rabbit anti-core protein IgG and then with donkey anti-rabbit IgG polyclonal antibody (Fab fragment, labeled with HRP; Dako, Glostrup, Denmark). The HRP label was amplified with FITC-conjugated tyramide according to the manufacturer's instructions (Molecular Probes, Eugene, OR). To detect human hepatocytes, liver sections were probed with anti-human hepatocyte monoclonal antibody (Dako), followed by anti-mouse IgG-Alexa 546 (Molecular Probes). Nuclei were stained by DAPI. Normal rabbit IgG was used as a control.

Transgenic mice with persistent HCV protein expression. To provide an immunocompetent model for inhibition of HCV protein expression, a mouse strain harbouring an HCV transgene was generated via a Cre/loxP switching system[37]. We bred CN2-29 transgenic mice, which carry an HCV transgene (nt. 294–3435), with Mx1-Cre transgenic mice, which express Cre recombinase in response to interferon (IFN)-α or a chemical inducer of IFN-α, poly(I:C). Following poly(I:C) injection, the HCV transgene was rearranged, and HCV sequences were expressed in the livers. In this model, HCV structure proteins are expressed in the liver within 7 days after poly(I:C) injection. Male CN2-29 trasgegenic mice (8–9 week-old) were injected intraperitoneally with 0.3 mL of 1 mg/mL poly(I:C) solution [in PBS (-)]. At 6 months after the poly(I:C) injection, the CN2-29 mice were administrated intravenously twice with the siRNA-MEND complex solution [1 mg/mL in PBS(-)] via orbital sinus at day 0 and day 2. The mice were sacrifice under anesthesia with ketamine/xylazine 2 days after the second siRNA-MEND administration. Livers were removed, fixed in 10% buffered formalin, and embedded in paraffin. Section (4 μm) were stained with hematoxylin and eosin, and observed using ZEISS Axio Imager A2 upright microscope (Carl Zeiss MicroImaging, Inc, Germany).

Statistical analysis. The data are expressed as the mean ± S.D. Statistical analysis of the difference between the HCV viral load during treatment and follow-up period and the baseline (day 0) level was conducted using the analysis of variance with a nonparametric Mann-Whitney U test. The probability values $P < 0.05$ were marked with *, and $P < 0.01$ were marked with **.

1. Hoofnagle, J. H. & Seeff, L. B. Peginterferon and ribavirin for chronic hepatitis C. *N Engl J Med* **355**, 2444–2451 (2006).
2. De Francesco, R. & Migliaccio, G. Challenges and successes in developing new therapies for hepatitis C. *Nature* **436**, 953–960 (2005).
3. Gao, M. *et al* Chemical genetics strategy identifies an HCV NS5A inhibitor with a potent clinical effect. *Nature* **465**, 96–100 (2010).
4. Elbashir, S. M., Harborth, J., Lendeckel, W., Yalcin, A., Weber, K. & Tuschl, T. Duplexes of 21-nucleotide RNAs mediate RNA interference in cultured mammalian cells. *Nature* **411**, 494–498 (2001).
5. Hannon, G. J. RNA interference. *Nature* **418**, 244–251 (2002).
6. Reynolds, A., Leake, D., Boese, Q., Scaringe, S., Marshall, W. S. & Khvorova, A. Rational siRNA design for RNA interference. *Nat Biotechnol* **22**, 326–330 (2004).
7. Ui-Tei, K. *et al.* Guidelines for the selection of highly effective siRNA sequences for mammalian and chick RNA interference. *Nucleic acids research* **32**, 936–948 (2004).
8. Patzel, V., Rutz, S., Dietrich, I., Koberle, C., Scheffold, A. & Kaufmann, S. H. Design of siRNAs producing unstructured guide-RNAs results in improved RNA interference efficiency. *Nat Biotechnol* **23**, 1440–1444 (2005).
9. Ameres, S. L., Martinez, J. & Schroeder, R. Molecular basis for target RNA recognition and cleavage by human RISC. *Cell* **130**, 101–112 (2007).
10. Tafer, H. *et al.* The impact of target site accessibility on the design of effective siRNAs. *Nat Biotechnol* **26**, 578–583 (2008).
11. Das, A. T. *et al.* Human immunodeficiency virus type 1 escapes from RNA interference-mediated inhibition. *J Virol* **78**, 2601–2605 (2004).
12. Konishi, M. *et al.* siRNA-resistance in treated HCV replicon cells is correlated with the development of specific HCV mutations. *J Viral Hepat* **13**, 756–761 (2006).
13. Wilson, J. A., Richardson, C. D. & Hepatitis, C. virus replicons escape RNA interference induced by a short interfering RNA directed against the NS5b coding region. *J Virol* **79**, 7050–7058 (2005).
14. Naito, Y., Ui-Tei, K., Nishikawa, T., Takebe, Y. & Saigo, K. siVirus: web-based antiviral siRNA design software for highly divergent viral sequences. *Nucleic acids research* **34**, W448–450 (2006).
15. Westerhout, E. M., Ooms, M., Vink, M., Das, A. T. & Berkhout, B. HIV-1 can escape from RNA interference by evolving an alternative structure in its RNA genome. *Nucleic acids research* **33**, 796–804 (2005).
16. Brown, K. M., Chu, C. Y. & Rana, T. M. Target accessibility dictates the potency of human RISC. *Nat Struct Mol Biol* **12**, 469–470 (2005).
17. Overhoff, M. *et al.* Local RNA target structure influences siRNA efficacy: a systematic global analysis. *J Mol Biol* **348**, 871–881 (2005).
18. Gredell, J. A., Berger, A. K. & Walton, S. P. Impact of target mRNA structure on siRNA silencing efficiency: A large-scale study. *Biotechnol Bioeng* **100**, 744–755 (2008).
19. de Fougerolles, A., Vornlocher, H. P., Maraganore, J. & Lieberman, J. Interfering with disease: a progress report on siRNA-based therapeutics. *Nat Rev Drug Discov* **6**, 443–453 (2007).
20. Kogure, K., Akita, H., Yamada, Y. & Harashima, H. Multifunctional envelope-type nano device (MEND) as a non-viral gene delivery system. *Adv Drug Deliv Rev* **60**, 559–571 (2008).
21. Sato, Y., Hatakeyama, H., Sakurai, Y., Hyodo, M., Akita, H. & Harashima, H. A pH-sensitive cationic lipid facilitates the delivery of liposomal siRNA and gene

silencing activity in vitro and in vivo. *Journal of controlled release: official journal of the Controlled Release Society* **163**, 267–276 (2012).
22. Connor, J., Yatvin, M. B. & Huang, L. pH-sensitive liposomes: acid-induced liposome fusion. *Proc Natl Acad Sci U S A* **81**, 1715–1718 (1984).
23. Straubinger, R. M., Duzgunes, N. & Papahadjopoulos, D. pH-sensitive liposomes mediate cytoplasmic delivery of encapsulated macromolecules. *FEBS Lett* **179**, 148–154 (1985).
24. Semple, S. C. *et al.* Rational design of cationic lipids for siRNA delivery. *Nat Biotechnol* **28**, 172–176 (2010).
25. Tsukiyama-Kohara, K., Iizuka, N., Kohara, M. & Nomoto, A. Internal ribosome entry site within hepatitis C virus RNA. *J Virol* **66**, 1476–1483 (1992).
26. Watanabe, T. *et al.* Intracellular-diced dsRNA has enhanced efficacy for silencing HCV RNA and overcomes variation in the viral genotype. *Gene Ther* **13**, 883–892 (2006).
27. Kim, D. H., Behlke, M. A., Rose, S. D., Chang, M. S., Choi, S. & Rossi, J. J. Synthetic dsRNA Dicer substrates enhance RNAi potency and efficacy. *Nat Biotechnol* **23**, 222–226 (2005).
28. Siolas, D. *et al.* Synthetic shRNAs as potent RNAi triggers. *Nat Biotechnol* **23**, 227–231 (2005).
29. Jinek, M. & Doudna, J. A. A three-dimensional view of the molecular machinery of RNA interference. *Nature* **457**, 405–412 (2009).
30. Arai, M. *et al.* Establishment of infectious HCV virion-producing cells with newly designed full-genome replicon RNA. *Arch Virol* **156**, 295–304 (2011).
31. Pei, Y. & Tuschl, T. On the art of identifying effective and specific siRNAs. *Nat Methods* **3**, 670–676 (2006).
32. Naito, Y., Yoshimura, J., Morishita, S. & Ui-Tei, K. siDirect 2.0: updated software for designing functional siRNA with reduced seed-dependent off-target effect. *BMC Bioinformatics* **10**, 392 (2009).
33. Akinc, A. *et al.* A combinatorial library of lipid-like materials for delivery of RNAi therapeutics. *Nat Biotechnol* **26**, 561–569 (2008).
34. Mercer, D. F. *et al.* Hepatitis C virus replication in mice with chimeric human livers. *Nat Med* **7**, 927–933 (2001).
35. Inoue, K. *et al.* Evaluation of a cyclophilin inhibitor in hepatitis C virus-infected chimeric mice in vivo. *Hepatology* **45**, 921–928 (2007).
36. Tsukiyama-Kohara, K. *et al.* Activation of the CKI-CDK-Rb-E2F pathway in full genome hepatitis C virus-expressing cells. *J Biol Chem* **279**, 14531–14541 (2004).
37. Sekiguchi, S. *et al.* Immunization with a recombinant vaccinia virus that encodes nonstructural proteins of the hepatitis C virus suppresses viral protein levels in mouse liver. *PLoS One* **7**, e51656 (2012).
38. Hutvagner, G. & Simard, M. J. Argonaute proteins: key players in RNA silencing. *Nat Rev Mol Cell Biol* **9**, 22–32 (2008).
39. MacRae, I. J., Ma, E., Zhou, M., Robinson, C. V. & Doudna, J. A. In vitro reconstitution of the human RISC-loading complex. *Proc Natl Acad Sci U S A* **105**, 512–517 (2008).
40. Yan, X. *et al.* The role of apolipoprotein E in the elimination of liposomes from blood by hepatocytes in the mouse. *Biochem Biophys Res Commun* **328**, 57–62 (2005).
41. Akinc, A. *et al.* Targeted delivery of RNAi therapeutics with endogenous and exogenous ligand-based mechanisms. *Mol Ther* **18**, 1357–1364 (2010).
42. Jacobs, F., Wisse, E. & De Geest, B. The role of liver sinusoidal cells in hepatocyte-directed gene transfer. *Am J Pathol* **176**, 14–21 (2010).
43. Sakurai, Yea. Gene Silencing via RNAi and siRNA quantification in Tumor Tissue using MEND, a Liposomal siRNA Delivery System. *Mol Ther* **in press**, (2013).
44. Jayaraman, M. *et al.* Maximizing the potency of siRNA lipid nanoparticles for hepatic gene silencing in vivo. *Angew Chem Int Ed Engl* **51**, 8529–8533 (2012).
45. Takahashi, M. *et al.* In vitro optimization of 2′-OMe-4′-thioribonucleoside-modified anti-microRNA oligonucleotides and its targeting delivery to mouse liver using a liposomal nanoparticle. *Nucleic acids research* **41**, 10659–10667 (2013).
46. Hatakeyama, H. *et al.* The systemic administration of an anti-miRNA oligonucleotide encapsulated pH-sensitive liposome results in reduced level of hepatic microRNA-122 in mice. *Journal of controlled release: official journal of the Controlled Release Society* **173**, 43–50 (2014).
47. Sakamoto, H. *et al.* Host sphingolipid biosynthesis as a target for hepatitis C virus therapy. *Nat Chem Biol* **1**, 333–337 (2005).
48. Wakita, T. *et al.* Production of infectious hepatitis C virus in tissue culture from a cloned viral genome. *Nat Med* **11**, 791–796 (2005).
49. Yasui, F., Sudoh, M., Arai, M. & Kohara, M. Synthetic lipophilic antioxidant BO-653 suppresses HCV replication. *J Med Virol* **85**, 241–249 (2013).
50. Honda, M., Beard, M. R., Ping, L. H. & Lemon, S. M. A phylogenetically conserved stem-loop structure at the 5′ border of the internal ribosome entry site of hepatitis C virus is required for cap-independent viral translation. *J Virol* **73**, 1165–1174 (1999).

Acknowledgments

We are very grateful to Dr. Fumihiko Yasui for his helpful discussion. This work was supported in part by grants from the Ministry of Education, Culture, Sports, Science and Technology (MEXT) of Japan; the Program for Promotion of Fundamental Studies in Health Sciences of Pharmaceuticals and Medical Devices Agency of Japan; the Ministry of Health, Labor and Welfare of Japan; the Special Education and Research Expenses of MEXT of Japan; and a Grant-in-Aid for Scientific Research on Innovative Areas "Nanomedicine Molecular Science" (No. 2306) from MEXT of Japan.

Author contributions

M.K. conceived the study. T.W., H.H., C.M. and Y.S. conducted the study equally. T.W. and H.H. coordinated the analysis and manuscript preparation. M.S. and H.H. had input into the study design and A.T., Y.H. and T.O. accomplished mouse management. M.A. and K.I. revised the manuscript for intellectual content. T.W., H.H., C.M. and Y.S. contributed equally.

Additional information

Supplementary information accompanies this paper at http://www.nature.com/scientificreports

Competing financial interests: Sudoh M. is an employee of Chugai Pharmaceutical Co., Ltd. Arai M. is an employee of Mitsubishi Tanabe Pharma Co., Ltd. The other authors disclose no conflicts.

How to cite this article: Watanabe, T. *et al. In vivo* therapeutic potential of Dicer-hunting siRNAs targeting infectious hepatitis C virus.. *Sci. Rep.* **4**, 4750; DOI:10.1038/srep04750 (2014).

Biochemical and Biophysical Research Communications 448 (2014) 56–62

Contents lists available at ScienceDirect

Biochemical and Biophysical Research Communications

journal homepage: www.elsevier.com/locate/ybbrc

Resistance to cyclosporin A derives from mutations in hepatitis C virus nonstructural proteins

Masaaki Arai [a,b], Kyoko Tsukiyama-Kohara [c,d], Asako Takagi [b], Yoshimi Tobita [b], Kazuaki Inoue [e], Michinori Kohara [b,*]

[a] Advanced Medical Research Laboratory, Mitsubishi Tanabe Pharma Corporation, 1000 Kamoshida-cho, Aoba-ku, Yokohama, Kanagawa 227-0033, Japan
[b] Department of Microbiology and Cell Biology, Tokyo Metropolitan Institute of Medical Science, Tokyo, Japan
[c] Transboundary Animal Diseases Centre, Joint Faculty of Veterinary Medicine, Kagoshima University, Kagoshima, Japan
[d] Laboratory of Animal Hygiene, Joint Faculty of Veterinary Medicine, Kagoshima University, Kagoshima, Japan
[e] Division of Gastroenterology, Showa University Fujigaoka Hospital, 1-30, Aoba-ku, Fujigaoka, Yokohama 227-8501, Japan

ARTICLE INFO

Article history:
Received 1 April 2014
Available online 19 April 2014

Keywords:
Hepatitis C virus
Cyclosporine A
Cyclophylin inhibitor
Mutation
Debio-025

ABSTRACT

Cyclosporine A (CsA) is an immunosuppressive drug that targets cyclophilins, cellular cofactors that regulate the immune system. Replication of hepatitis C virus (HCV) is suppressed by CsA, but the molecular basis of this suppression is still not fully understood. To investigate this suppression, we cultured HCV replicon cells (Con1, HCV genotype 1b, FLR-N cell) in the presence of CsA and obtained nine CsA-resistant FLR-N cell lines. We determined full-length HCV sequences for all nine clones, and chose two (clones #6 and #7) of the nine clones that have high replication activity in the presence of CsA for further analysis. Both clones showed two consensus mutations, one in NS3 (T1280V) and the other in NS5A (D2292E). Characterization of various mutants indicated that the D2292E mutation conferred resistance to high concentrations of CsA (up to 2 μM). In addition, the missense mutation T1280V contributed to the recovery of colony formation activity. The effects of these mutations are also evident in two established HCV replicon cell lines—HCV-RMT ([1], genotype 1a) and JFH1 (genotype 2a). Moreover, three other missense mutations in NS5A—D2303H, S2362G, and E2414K—enhanced the resistance to CsA conferred by D2292E; these double or all quadruple mutants could resist approximately 8- to 25-fold higher concentrations of CsA than could wild-type Con1. These four mutations, either as single or combinations, also made Con1 strain resistant to two other cyclophilin inhibitors, N-methyl-4-isoleucine-cyclosporin (NIM811) or Debio-025. Interestingly, the changes in IC_{50} values that resulted from each of these mutations were the lowest in the Debio-025-treated cells, indicating its highest resistant activity against the adaptive mutation.

1. Introduction

The genome of the hepatitis C virus (HCV) is a single-stranded RNA with positive polarity and is classified in the *Flaviviridae* family. HCV frequently establishes chronic infections that lead to liver cirrhosis and hepatocellular carcinoma (HCC) [2]. An estimated 130–200 million people worldwide are now infected with HCV [3]. HCVs have been classified into six major genotypic groups (genotypes 1–6); genotype 1 is the most prevalent over most of the world. Treatments with alpha interferon (IFNα), together with the nucleoside analog ribavirin (RBV), greatly increased the percentage of HCV chronically infected patients able to reach a sustained anti-viral response (SVR). Covalent attachment of polyethylene glycol (PEGylated) IFN-α-plus-RBV therapy has a success rate of ~80% in patients with genotype 2 or 3 infections, but only ~50% in patients with genotype 1 infections [4,5]. The recently approved protease inhibitors boceprevir and telaprevir each improved the efficacy of IFN-α-plus-RBV therapy [6]. These direct-acting agents (boceprevir, simeprevir, sofosbuvir, faldaprevir and telaprevir, etc.) each have the advantage of being highly specific, but each may select for specific resistant mutations, limiting their long-time efficacy. Therefore, antiviral inhibitors targeting host factors crucial for viral replication should be developed to overcome these problems.

Abbreviations: HCV, hepatitis C virus; CsA, cyclosporine A; HCC, hepatocellular carcinoma; IFNα, alpha interferon; Cyp, cyclophilins; SVR, sustained anti-viral response.

* Corresponding author. Address: Department of Microbiology and Cell Biology, Tokyo Metropolitan Institute of Medical Science, 2-1-6, Kamikitazawa, Setagaya-ku, Tokyo 156-8506, Japan. Fax: +81 3 5316 3137.
E-mail address: kohara-mc@igakuken.or.jp (M. Kohara).

http://dx.doi.org/10.1016/j.bbrc.2014.04.053
0006-291X/

Reportedly, several HCV proteins interact with cyclophilins (Cyp) and modulate HCV replication [7–9]. To date, three Cyp inhibitors—Debio-025, NIM811, and SCY-635—have been deemed safe and effective for patients with HCV in phase I and II studies [10–12]. Development of Debio-025 has advanced the farthest through phase II studies, and Debio-025 has approved and showed a great deal of promise for decreasing HCV viremia in infected patients. However, emergence of drug-resistant HCV mutants could limit the therapeutic potential of CsA and Cyp inhibitors.

The HCV genome is a positive-sense, single-stranded RNA (about 9.6 kb) that encodes at least 10 viral proteins; these are categorized as structural core proteins (E1, E2) or nonstructural (p7, NS2, NS3, NS4A, NS4B, NS5A, and NS5B) [13,14]. The nonstructural proteins are involved in HCV RNA replication [14]. NS5A protein comprises three domains linked by two low-complexity sequences (LCS) that are either serine or proline rich; domain I is a highly structured zinc binding domain whose three-dimensional structure shows two dimeric conformations [15,16]. Domains II and III have been shown to be unstructured in their native states, but nuclear magnetic resonance and circular dichroism have shown that elements of secondary structure run throughout each of these domains [17–19]. NS5A is anchored to membranes by an N-terminal amphipathic helix and is an essential component of the viral genome replication complex; it also interacts with other non-structural proteins [20] or cellular factors. NS5A domain II is a substrate for the peptidyl-prolyl cis/trans isomerase activity of Cys A and B [21], and NS5A domain III is reportedly a substrate of CypA [22].

In this study, we used CsA to select for and isolate drug-resistant HCV mutants; we then performed virus genome sequencing to investigate the molecular mechanisms of this drug resistance.

2. Materials and methods

2.1. Cells, electroporation and ethics statement

HuH-7 cells were cultured in DMEM-GlutaMax-I (Invitrogen, Carlsbad, CA, USA) supplemented with 10% fetal bovine serum, penicillin, and streptomycin (Invitrogen). Replicon cells were maintained in the same medium supplemented with 300 μg/ml G418 (Invitrogen). Cells were passaged three times a week, and at each passage, each culture was split into four subcultures. Electroporation of replicon RNA and G418 selection were performed as previously described [23]. All experimental protocol was approved by the regional research institute.

2.2. Establishment of cyclosporin A resistant replicon clones

FLR3-1 cells derived from Con1 (AJ238799)-based, luciferase-harboring HCV sub-genomic replicon cell were treated with both 2 μM of cyclosporin A and 0.5 mg/ml of G418 for 24 days. Surviving cells were further treated with 3 μM CsA for 2 days, 4 μM for 4 another days, and finally 6 μM for the last 10 days. Using limiting dilution cloning, we established nine clonal cell lines. Using real-time RT-PCR (ABI 7700 system, Applied Biosystems, Foster City, CA, USA) as described previously [24], we systematically measured HCV RNA copy number in each of these nine clonal lines.

2.3. Determination of consensus sequence of resistant clones

LongRange Reverse transcriptase (QIAGEN, Valencia, CA, USA) and an oligonucleotide primer (antisense sequence 9549–9569 of HCV-Con1) were used to reverse transcribe purified RNA (1 μg). The resulting cDNA, Phusion DNA polymerase (Finnzymes, Vantaa, Finland), and primers recognizing each non-coding region were used for PCR amplification of the entire non structural protein coding region of the sub-genomic replicon. The TA cloning kit (Invitrogen) was used to introduce each fragment into a separate plasmid; we picked up eight clones from each resistant cell line and their nucleotide sequences were determined.

2.4. Construction and RNA transcription

The pFK I389neo/NS3-3′/5.1 and pFK I389luc/NS3-3′/5.1 plasmids (ReBlikon, Baden-Württemberg, Germany) were used to generate HCV constructs with regions of the sub-genomic replicon with mutations (Fig. 2A). The QuikChangeII kit (Stratagene, La Jolla, CA, USA) was used to introduce specific mutations into the HCV sequences. To generate RNA, plasmids were digested with *XbaI* and used as a template for RNA transcription; RiboMax (Promega, Madison, WI, USA) was used for each transcription reaction.

2.5. Drug treatment

For the drug resistance assays, established CsA-resistant replicon clones were seeded onto 24-well tissue culture plates (10,000 cells/well) and cultivated overnight. Then cells were treated with various concentrations of CsA (0–8 μM) for 4 days. Surviving cells were stained with crystal violet.

For HCV replication inhibition assays, replicon cells were seeded in 96-well tissue culture plates (5000 cells/well) and cultivated overnight. Serial dilutions of CsA (Fluka Chemie, Buchs, Switzerland) or NIM811 (Novartis) and Debio025 (Debiopharma) were then added to sets of wells. After incubation for 72 h, ABI prizm 6100 (Applied Biosystems) was used to extract total RNA from cells, and HCV-RNA was measured as described above. Each assay was carried out in triplicate.

For another HCV replication inhibition assay, mutant replicon RNA derived from pFK I389luc/NS3-3′/5.1 plasmid were introduced into HuH7 cells via electroporation, and the transformed/transfected cells were seeded to 96-well tissue culture plates. Drugs were added 24 h after electroporation. Luciferase activities were evaluated 4 h or 72 h after electroporation, which corresponded to 20 h before drug treatment or 48 h after drug treatment, respectively; the Blight-Glo kit (Invitrogen) and Envision (Perkin Elmer, Waltham, MA, USA) were used to take all measurements, and values at 72 h were normalized relative to the values from 4 h.

3. Results

3.1. Establishment of CsA-resistant clones

To establish CsA-resistant clones, we treated HCV FLR-N replicon cells with CsA (Fig. 1A) and obtained nine resistant clonal cell lines. We measured the amount of HCV RNA in each resistant clonal line and chose for further study the three lines that consistently had the largest amount of HCV RNA (Fig. 1B). We then determined the entire HCV sequence from 16 subclones; we isolated two groups of eight subclones (one group each from clones #6 and #7), because we could not establish clone #2; each subclone was isolated by treating a CsA-resistant clone (#6 or #7) with 6 μM CsA (Table 1). Although there were several mutations in the NS3–NS5B protein-coding regions, common mutations were isoleucine (I) to valine (V) at amino acid 1280 (T1280V) and aspartic acid (D) to glutamic acid (E) at amino acid 2292 (D2292E). At 1280, original Con1 has threonine (T) and was mutated into (I) in Con1 replicon cells.

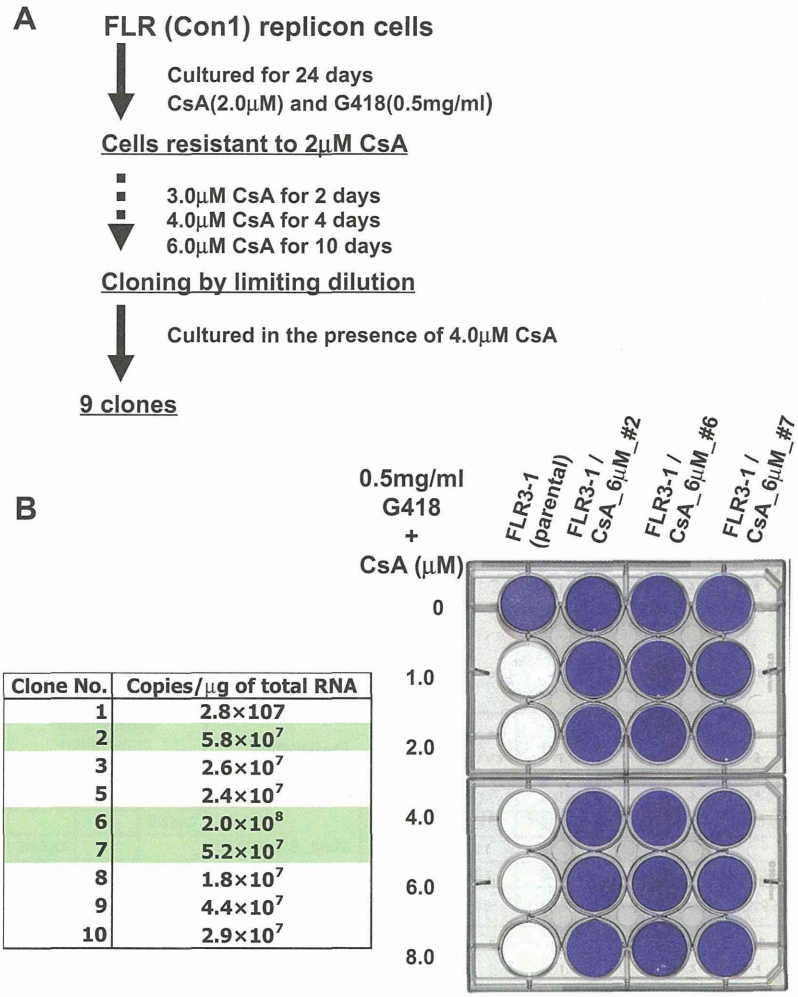

Clone No.	Copies/μg of total RNA
1	2.8×107
2	5.8×10^{7}
3	2.6×10^{7}
5	2.4×10^{7}
6	2.0×10^{8}
7	5.2×10^{7}
8	1.8×10^{7}
9	4.4×10^{7}
10	2.9×10^{7}

Fig. 1. Basic characteristics of the nine cyclosporin A-resistant clones. (A) Flow chart outlining the selection of cyclosporin A-resistant HCV replicon clones. (B) Real-time PCR was used to determine the copy number of each Cys A-resistant clone. The three clones with the highest HCV genome copy number are highlighted in green (Left). Colony formation assay of mutant #2, 6 and 7 (Right). (For interpretation of the references to color in this figure legend, the reader is referred to the web version of this article.)

3.2. Identification of mutations responsible for CsA resistance

To define the mutations responsible for CsA resistance, we constructed various chimeric clones that each contained specific mutation that arose from CsA selection (Fig. 2A). We could thereby evaluate each mutation with regard to its effect on CsA resistance. We found that mutations in two proteins—NS5A and NS4A—significantly enhanced the resistance against CsA treatment (Fig. 2B). We also cultured replicon cells with these mutants in the presence of CsA (up to 2 μM); we found that cells with a D2292E mutation could survive, but cells with wild-type NS5A or T1280V mutation could not (Fig. 3A).

The effect of T1280V mutation on colony formation was further evaluated (Fig. 3B). Introduction of the T1280V mutation in *cis* to the D2292E mutation rescued the colony-formation defect of the D2292E mutant replicon cells; specifically, the T1280V–D2292E double-mutant replicon cells had the same colony-forming ability as the parental replicon cells.

3.3. Evaluation of mutations for CsA resistance in other HCV genotypes

We evaluated whether the mutations that conferred CsA resistance to the HCV Con1 strain (genotype 1b) also conferred CsA resistance to the RMT (genotype 1a; AB520610) and JFH1 (genotype 2a; AB047639) strains (Fig. 4A, B and Table 2) [1]. D2292E conferred CsA resistance to the HCV strains RMT and JFH1, but T1280V did not (Table 2), as observed with HCV Con1 strain (Fig. 2E). The amino acid sequences surrounding mutations other than D2292E showed some differences among three genotypes (1a, 1b, and 2a) (Fig. 4B). D2292E mutants of these three genotypes showed resistance to CsA (Fig. 2E, Table 2) but the fold increase of resistance in genotype 1a and 2a was lower than that of genotype 1b (Tables 2 and 3). Therefore, there might be some residue(s) other than D2292E to influence the resistance to CsA.

3.4. Efficacy of mutations in NS5A for conferring CsA resistance

Although D2292E clearly conferred CsA resistance to HCV, other mutations in NS5A may also have had an effect because constructs with all four of the original NS5A mutations found in clone #6 mutations were more resistant to CsA than were constructs with only the D2292E mutation (Fig. 2B and E). We constructed HCV-luciferase replicons, each with one or more of four mutations (D2292E, D2303H, S2362G, and E2414K). HuH-7 cells were transiently transfected with RNA of each construct; we then treated the transfected cells with CsA (Table 3). Of the four single mutants, all but S2362G conferred some CsA resistance to HCV-luciferase replicons; notably, combinations of mutations had additive effects

A

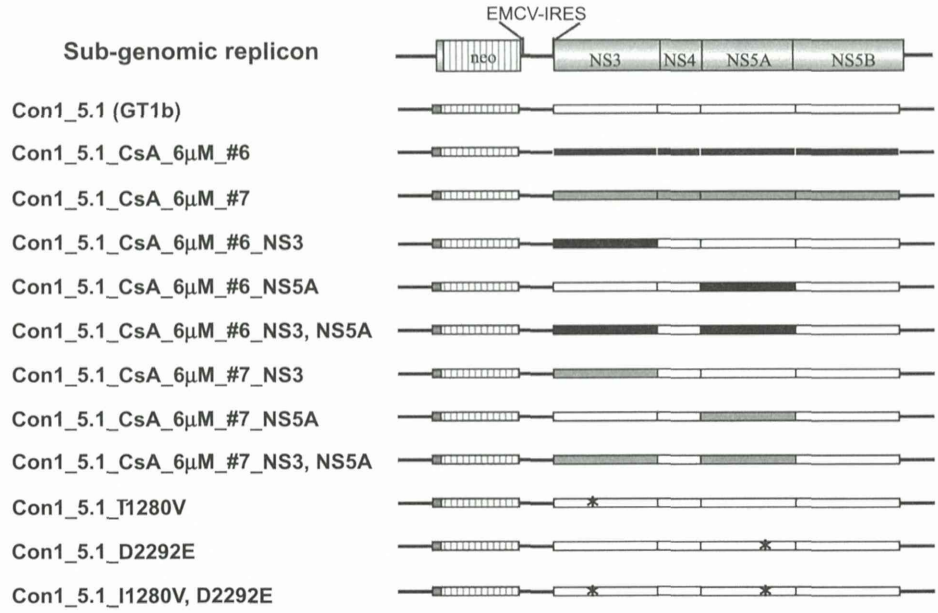

B

Cyclosporin A	Replacement or Mutation			IC_{50} (μM)	Fold change
	NS3	NS4A	NS5A		
Con1_5.1 (GT1b)	-	-	-	0.18	1.0
	Cs6#6	-	-	0.21	1.2
	-	-	Cs6#6	2.10	11.7
	Cs6#6	-	Cs6#6	2.20	12.2
	Cs6#6	V1681A	Cs6#6	5.40	30.0

C

NIM811	replacement or mutations			IC_{50} (μM)	Fold change
	NS3	NS4A	NS5A		
Con1_5.1 (GT1b)	-	-	-	0.09	1.0
	Cs6#6	-	-	0.10	1.1
	-	-	Cs6#6	0.49	5.4
	Cs6#6	-	Cs6#6	0.50	5.6
	Cs6#6	V1681A	Cs6#6	1.80	20.0

D

Debio025	Replacement or mutation			IC_{50} (μM)	Fold change
	NS3	NS4A	NS5A		
Con1_5.1 (GT1b)	-	-	-	0.05	1.0
	Cs6#6	-	-	0.04	0.8
	-	-	Cs6#6	0.43	7.8
	Cs6#6	-	Cs6#6	0.40	8.0
	Cs6#6	V1681A	Cs6#6	0.75	13.7

E

Cyclosporin A	Replacement or mutation			IC_{50} (μM)	Fold change
	NS3	NS4B	NS5A		
Con1_5.1 (GT1b)	-	-	-	0.54	1.0
	Cs6#7	-	-	0.59	1.1
	-	-	Cs6#7	2.36	4.4
	Cs6#7	-	Cs6#7	2.51	4.6
	Cs6#7	I1797V	Cs6#7	2.44	4.5
	T1280V	-	-	0.57	1.1
	-	-	D2292E	1.71	3.1
	T1280V	-	D2292E	1.76	3.3

Fig. 2. (A) Schematic representations of 12 Con1 replicon-derived constructs. (B–D) Evaluation of Cs6#6 constructs with regard to resistance to CsA or to each of two CsA derivatives (NIM811 and Debio025). Real-time PCR was used to measure HCV sub-genome copy number in cells, and IC_{50}s were then determined from the copy number values. For each construct, the fold change represents the ratio of IC_{50} values from the construct and the parental Con1 replicon (IC50Construct:IC50Parental). (E) Resistance to CsA of three Cs6#7 derivative constructs that represent the T1280V and D2292E mutations as each single mutation or as a double mutation.

and conferred greater CsA resistance than any single mutation. The HCV replicon with all four mutations showed the strongest CsA resistance.

3.5. Evaluation of CsA-resistant mutants for resistance to cyclophilin inhibitors

We further evaluated each of the NS5A mutants for their ability to confer resistance to each of two other cyclophilin inhibitors, N-methyl-4-isoleucine-cyclosporin (NIM811, Table 4) and Debio-025 (Table 5). Of the four single mutants, D2292E conferred the highest resistance, and the combination of all four mutations conferred the overall highest resistance to NIM811 and to Debio-025. When we compared CsA, NIM811, and Debio-025, the mutation-mediated increases in IC_{50} values were lowest with the Debio-025 treatment (Tables 3–5).

4. Discussion

Here, we investigated two of nine HCV sub-genomic replicon cell clones (CsA-resistant HCV mutants) isolated following long-term dual treatment with CsA and G418. Comparing the HCV sequences of these two clones (#6 and #7), only two of many mutant sites were shared between the mutant HCV sequences. Specifically, both clones #6 and #7 had a D2292E missense mutation in NS5A and a T1280V missense mutation in NS3. D2292E is